

Lattice vibrations in hexagonal Ga_{1-x}Mn_xN epitaxial films on *c*-plane sapphire substrates by infrared reflectance spectra

Z. G. Hu, M. Strassburg, A. Weeraseskara, N. Dietz, and A. G. U. Perera^{a)}
Department of Physics and Astronomy, Georgia State University, Atlanta, Georgia 30303

M. H. Kane,^{b)} A. Asghar, and I. T. Ferguson^{b)}
School of Electrical and Computer Engineering, Georgia Institute of Technology, Atlanta, Georgia 30332

(Received 19 August 2005; accepted 22 December 2005; published online 9 February 2006)

The lattice vibrations of undoped hexagonal Ga_{1-x}Mn_xN (*x* from 0.0% to 1.5%) epitaxial films grown on *c*-plane sapphire substrates by metalorganic chemical vapor deposition have been investigated using infrared reflectance spectra in the frequency region of 200–2000 cm⁻¹ (5–50 μm) at room temperature. The experimental reflectance spectra were analyzed using the Lorentz oscillator model for infrared-active phonon observed. The *E*₁(LO) phonon frequency slightly decreases with increasing Mn composition. However, the *E*₁(TO) phonon frequency linearly increases with the Mn composition, which can be well expressed by (558.7+350*x*) cm⁻¹ and the broadening values are found to be larger than that of the GaN film. It indicates that Mn incorporation decreases the peak values (from the *E*₁ phonon) of the infrared dielectric functions due to the local variation in the lattice constants and to the destruction of the crystal translational symmetry. © 2006 American Institute of Physics. [DOI: 10.1063/1.2172718]

The idea of utilizing the spin of carriers in novel spintronic devices has led to efforts in fabricating and investigating appropriate new semiconductor materials during the past years.^{1,2} Diluted magnetic semiconductors (DMS) based on III-V group semiconductors have attracted considerable interest as materials that can support the transport and storage of spin, and that can be integrated into existing electronic and optoelectronic devices.^{3–5} Among these DMS materials, manganese (Mn)-doped GaN (Ga_{1-x}Mn_xN) epitaxial films attracted strong attention due to the theoretical prediction of room-temperature ferromagnetism in the nitrides using the Zener model.^{6,7} Experimental studies on the fundamental physical properties are still rare, however, there have been numerous reports of successful preparation of Ga_{1-x}Mn_xN films and their magnetic properties.^{4,8,9} Moreover, these reports mainly focused on the optical band gap energy and some important Mn (Mn²⁺, Mn³⁺, and Mn⁴⁺) level transition energies in the Ga_{1-x}Mn_xN films. The behavior of *E*₁ phonon modes (perpendicular to the *c*-axis) in these hexagonal materials, which are subject to local vibrational character,^{10,11} is particularly interesting because of the important effects from the Mn incorporation with the GaN matrix. The lattice vibrations and dielectric functions of the Ga_{1-x}Mn_xN films not only provide basic physical properties, but are also critical for developing the materials for optoelectronic device applications. Infrared (IR) reflectance spectroscopy is a nondestructive probe technique, which is an attractive and powerful tool for the optical characterization of semiconductor film materials. The *E*₁ phonon mode characteristics of hexagonal Al_xGa_{1-x}N films on silicon and sapphire substrates have been studied using IR reflectance spectra.^{10,11} Similarly, IR reflectance can also provide the information on the phonon modes of the Ga_{1-x}Mn_xN films.

In this letter, the lattice vibration properties of Ga_{1-x}Mn_xN epitaxial films deposited on sapphire substrates are investigated using IR reflectance spectra. Effects of Mn composition on the *E*₁ phonon modes and the dielectric functions are discussed in detail.

Hexagonal Ga_{1-x}Mn_xN epitaxial films in a composition range from 0.0% to 1.5% were grown on *c*-plane sapphire substrates by metalorganic chemical vapor deposition (MOCVD).⁴ The epilayers were deposited using a modified GaN MOCVD reactor with a vertical injection system. Initially, undoped GaN epilayers (sample A) were used as templates in order to obtain the mirror-like surfaces. Then Ga_{1-x}Mn_xN epitaxial films were deposited on the GaN templates. More details of the growth process can be found in Ref. 4. Near-normal reflectance spectra (~8°) were measured at room temperature (RT) over the frequency range of 200–2000 cm⁻¹ (5–50 μm) using a Fourier transform infrared (FTIR) spectrometer as described before.¹² The *s*-polarized incident light was used in order to predominantly identify the *E*₁ phonon behavior in this work.

Due to the reststrahlen regions of sapphire overlapping with those of Ga_{1-x}Mn_xN, and the interference effects in the transparent region, a model interpretation was applied to extract the phonon modes and dielectric functions of the Ga_{1-x}Mn_xN epilayers. For sample A, a three-phase model (air/GaN/sapphire) was used.¹² Thereafter, the fitting parameters obtained were kept constant in all subsequent four-phase model (air/Ga_{1-x}Mn_xN/GaN/sapphire) calculations for the Ga_{1-x}Mn_xN films. The *s*-polarized light reflectance was used to reproduce the experimental spectra. The reflectance of the multilayer stack was calculated using Maxwell's equations assuming each layer to be isotropic.¹² The isotropic treatments are reasonable for the phonon modes, which are perpendicular to the *c*-axis under near-normal incident configurations using the *s*-polarized light.¹⁰ Only the *E*₁ phonons are IR-active in the present measurements based on the selection rule. For polar semiconductor materials, IR dielectric functions of the Ga_{1-x}Mn_xN films can be written as

^{a)}Electronic mail: uperera@gsu.edu

^{b)}Present address: School of Materials Science and Engineering, Georgia Institute of Technology, Atlanta, GA 30332.

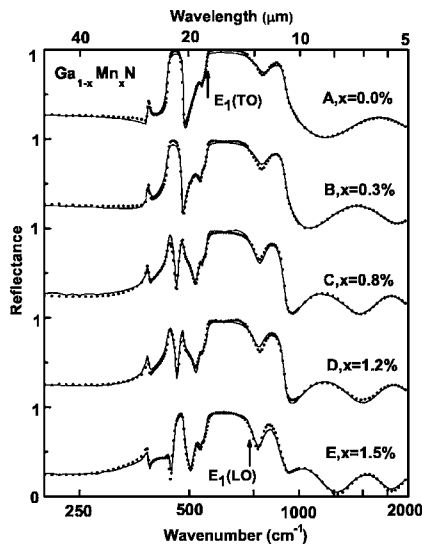


FIG. 1. Experimental infrared reflectance spectra (dotted lines) of the $\text{Ga}_{1-x}\text{Mn}_x\text{N}$ films on sapphire and their best fit results (solid lines). Each spectrum is successively shifted by 1.0 in the vertical direction. Every 10th point in the range $<380\text{ cm}^{-1}$ and $580\text{--}1000\text{ cm}^{-1}$, every other point in the range $380\text{--}580\text{ cm}^{-1}$, and every 40th point in the range $>1000\text{ cm}^{-1}$ in the experimental data are shown for clarity. The horizontal coordinate is the logarithmic unit to enlarge the reststrahlen region.

$$\varepsilon(\omega) = \varepsilon_{\infty} \left(1 + \frac{\omega_{\text{LO}}^2 - \omega_{\text{TO}}^2}{\omega_{\text{TO}}^2 - \omega^2 - i\omega\Gamma} \right). \quad (1)$$

Here, ε_{∞} , ω_{LO} , ω_{TO} , Γ , and ω represent, in order, the high-frequency dielectric constants, the longitudinal-optical (LO) phonon frequency, the transverse-optical (TO) phonon frequency, the broadening values of the $E_1(\text{TO})$ phonon and the incident light frequency. It should be noted that the free carrier effects are neglected since the $\text{Ga}_{1-x}\text{Mn}_x\text{N}$ epilayers are nominally undoped. High free carrier concentration was ruled out by Raman studies, providing an upper limit of 10^{16} cm^{-3} for doping, which was the detection limit of the applied Hall-effect measurements.⁵

The experimental reflectance spectra for the $\text{Ga}_{1-x}\text{Mn}_x\text{N}$ epilayers with the composition x varying from 0.0% to 1.5% are shown in Fig. 1 (dotted lines). The broadening edge at 910 cm^{-1} is assigned to the reststrahlen band of the sapphire, which is close to the LO phonon frequency of 909 cm^{-1} . The reflectance strength is very small (about 20%) for the epilayers below the frequency of 300 cm^{-1} , indicating further that the contributions from the free carriers need not be considered. An interference effect beyond 1000 cm^{-1} ($<10\text{ }\mu\text{m}$) is clearly observed for all films indicating that the epilayers are transparent in this region. For samples A and B, a sapphire like peak¹³ is seen around 450 cm^{-1} . This peak splits into two peaks for the epilayers with higher Mn compositions. For sample E, the second peak is much stronger, which maybe due to the local vibrations from Mn alloy. There is also a dip at about 785 cm^{-1} in the reflectance spectra of the epilayers. This is due to an interference within the subwavelength thickness of the $\text{Ga}_{1-x}\text{Mn}_x\text{N}$ epilayers on the highly reflecting sapphire and the exact position varies with the different thicknesses.¹⁰ The following simulations confirm this for the $\text{Ga}_{1-x}\text{Mn}_x\text{N}$ epilayers and give their respective thickness values.

The calculated reflectance spectra are also shown in Fig.

1 (solid lines). A good agreement between the calculated and

TABLE I. The parameter values of the Lorentz oscillator models were derived from the simulations to the infrared reflectance spectra of the $\text{Ga}_{1-x}\text{Mn}_x\text{N}$ films. The 90% confidence limits of the fitting parameters were given in brackets.

Samples	x (%)	Thickness (nm)	ε_{∞}	ω_{LO} (cm^{-1})	ω_{TO} (cm^{-1})	Γ (cm^{-1})
A	0.0	2102.6 (8.2)	5.08 (0.03)	746.4 (1.7)	558.4 (0.6)	5.0 (0.2)
B	0.3	366.5 (5.9)	5.18 (0.06)	747.2 (3.4)	560.0 (0.6)	7.0 (0.6)
C	0.8	1116.5 (6.5)	5.16 (0.04)	746.4 (1.8)	562.2 (0.8)	6.9 (0.3)
D	1.2	1051.0 (7.5)	5.25 (0.05)	740.8 (2.2)	562.5 (0.9)	7.0 (0.4)
E	1.5	1718.5 (8.8)	5.22 (0.04)	745.0 (1.3)	563.7 (0.8)	9.6 (0.3)

experimental data is obtained in the entire frequency region. However, the small deviations can be observed due to the local vibrations from incorporated Mn atoms, which are not considered in Eq. (1). A more rigorous dielectric function model based on the random phase approximation (RPA) has been recently presented by Aguado *et al.*³ However, the single oscillator model used in the present work still provides a good insight on the E_1 phonon modes observed. The best-fit parameters of the Lorentz oscillator model together with the fitting errors are listed in Table I. The thickness of the sample B with $x=0.3\%$ ($366.5 \pm 5.9\text{ nm}$) is the smallest compared to the other epilayers with thickness between ~ 1 and $\sim 2\text{ }\mu\text{m}$. The high-frequency dielectric constants ε_{∞} of the $\text{Ga}_{1-x}\text{Mn}_x\text{N}$ films vary from 5.08 ± 0.03 to 5.25 ± 0.05 , which are slightly below the reported value of 5.35 for GaN.¹¹ Figure 2(a) shows a composition dependency of the $E_1(\text{LO})$ phonon frequency which may be expressed in the form $(746.6 - 160x)\text{ cm}^{-1}$ with the Mn composition x . It shows that the $E_1(\text{LO})$ phonon slightly decreases with increasing Mn composition. However, the $E_1(\text{TO})$ phonon frequency increases with Mn composition as shown in Fig. 2(b). The results show a linear dependency of the $E_1(\text{TO})$ phonon frequency on the Mn composition range from 0.0% to 1.5%: $(558.7 + 350x)\text{ cm}^{-1}$. Limmer *et al.*² reported a similar linear dependency (a minute decreasing trend) for $\text{Ga}_{1-x}\text{Mn}_x\text{As}$ films with Mn compositions from 0.0% to 2.8%. The linear dependency maybe due to the local variation of the lattice constants for the $\text{Ga}_{1-x}\text{Mn}_x\text{N}$ films with different Mn compositions. Thaler *et al.*⁷ observed a linear decrease in the

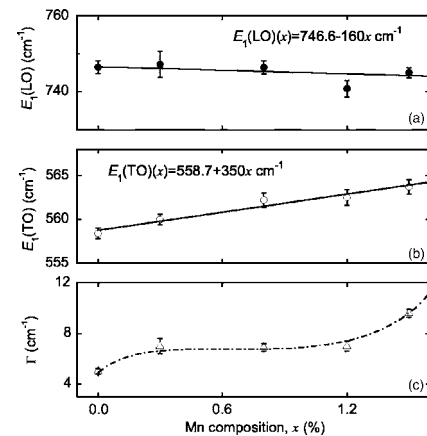


FIG. 2. Mn composition dependence of (a) the $E_1(\text{LO})$ phonon frequency, (b) the $E_1(\text{TO})$ phonon frequency, and (c) the broadening value of the $E_1(\text{LO})$ phonon for the $\text{Ga}_{1-x}\text{Mn}_x\text{N}$ films. The solid lines in (a) and (b) represent the linear fitting results. The dashed line in (c) is only used to guide the eye.

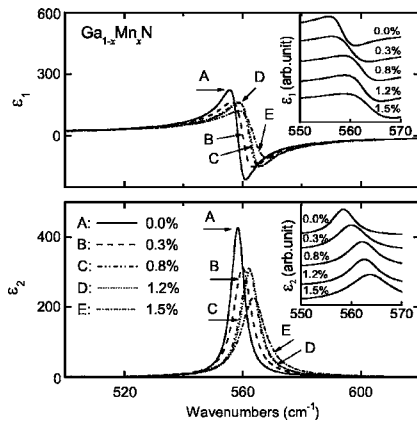


FIG. 3. The infrared dielectric functions of the $\text{Ga}_{1-x}\text{Mn}_x\text{N}$ films with different Mn compositions. ϵ_1 and ϵ_2 are the real and imaginary parts of the dielectric functions, respectively. The inset is an enlargement of the $E_1(\text{TO})$ phonon mode region.

lattice constant as the Mn composition increases from 0.0% to 3.0%. A similar structural change might be induced in the $\text{Ga}_{1-x}\text{Mn}_x\text{N}$ layers. IR reflectometry is better than Raman spectrometry for the study of the E_1 phonon modes because the close proximity of the E_2 (high) phonon mode at 569 cm^{-1} and its strong intensity¹⁴ limits the resolution in Raman studies. The broadening values of the $E_1(\text{TO})$ phonon show a slightly increasing trend (from 5.0 to 9.6 cm^{-1}) with the composition [Fig. 2(c)]. Note that the values are nearly the same for the films with $x=0.3, 0.8,$ and 1.2 . It indicates that the crystalline quality does not significantly change with the Mn concentrations studied so far. The Mn alloy reduces the bonding forces in the material and weakens the translational symmetry of the crystal lattice, which leads to a slight broadening of the $E_1(\text{TO})$ phonon line.²

Figure 3 shows IR dielectric functions for the E_1 phonon modes of the $\text{Ga}_{1-x}\text{Mn}_x\text{N}$ epitaxial films with the Mn composition, x in the frequency region of $500\text{--}620\text{ cm}^{-1}$ ($16\text{--}20\text{ }\mu\text{m}$). In the transparent region (below 500 cm^{-1}), the real part ϵ_1 of the dielectric function is 4.8 indicating the refractive index is about 2.2, which is closer to the reported values (2.2–2.3) obtained from the transmission spectra of GaN.¹⁵ The peak position of the imaginary part [correspondingly to the $E_1(\text{TO})$ phonon] shows a blueshift trend with increasing Mn composition. Moreover, the line shapes of the $\text{Ga}_{1-x}\text{Mn}_x\text{N}$ films are obviously different from that of the GaN film in the reststrahlen region (see the inset of Fig. 3) and become more broadened. As discussed above, the peak value of the GaN film is larger due to a smaller broadening value (5.0 cm^{-1}). From this viewpoint, it can be also found that the effects from Mn alloy are significant for the properties of the E_1 phonon modes. In addition, the dielectric functions are the basic parameters for FIR detector designs. The total absorption of detectors based on the $\text{Ga}_{1-x}\text{Mn}_x\text{N}$ materials can be calculated using the obtained dielectric functions. At the wavelength of $20\text{ }\mu\text{m}$, the absorption coefficient of undoped $\text{Ga}_{1-x}\text{Mn}_x\text{N}$ films is about 10^3 cm^{-1} , which is much larger than the value (500 cm^{-1}) of the GaN film as shown in Fig. 4. It indicates that the introduction of Mn increases the absorption coefficient for the $\text{Ga}_{1-x}\text{Mn}_x\text{N}$ films in the FIR region. The results keep the promise for the designs of novel GaMnN/GaN FIR detectors.¹⁶

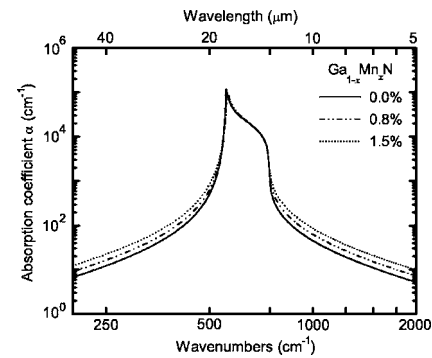


FIG. 4. The infrared absorption coefficients of the $\text{Ga}_{1-x}\text{Mn}_x\text{N}$ films with Mn composition 0.0% (solid line), 0.8% (dashed-dotted line), and 1.5% (dotted line) from the dielectric functions.

In conclusion, the infrared optical properties of hexagonal $\text{Ga}_{1-x}\text{Mn}_x\text{N}$ ($0.0\% \leq x \leq 1.5\%$) films deposited on sapphire substrates have been investigated using IR reflectance spectroscopy. The $E_1(\text{LO})$ phonon frequency decreases and the $E_1(\text{TO})$ phonon frequency linearly increases with the Mn composition. The dielectric functions of the $\text{Ga}_{1-x}\text{Mn}_x\text{N}$ films are slightly below those in GaN film in the reststrahlen region indicating a weakening of the local structural bonding in the wurtzite lattice due to Mn introduction.

The work was supported in part by the U.S. NSF under Grant No. ECS-0140434. M.S. acknowledges the support from the Alexander von Humboldt foundation. M.H.K. received support through the National Defense Science and Engineering Graduate Fellowship.

- ¹T. Dietl, H. Ohno, F. Matsukura, J. Cibert, and D. Ferrand, *Science* **287**, 1019 (2000).
- ²W. Limmer, M. Glunk, S. Mascheck, A. Koeder, D. Klarer, W. Schoch, K. Thonke, R. Sauer, and A. Waag, *Phys. Rev. B* **66**, 205209 (2002).
- ³R. Aguado, M. P. López-Sancho, J. Sinova, and L. Brey, *Phys. Rev. B* **70**, 195201 (2004).
- ⁴M. H. Kane, A. Asghar, C. R. Vestal, M. Strassburg, J. Senawiratne, Z. J. Zhang, N. Dietz, C. J. Summers, and I. T. Ferguson, *Semicond. Sci. Technol.* **20**, L5 (2005).
- ⁵M. H. Kane, A. Asghar, A. M. Payne, C. R. Vestal, Z. J. Zhang, M. Strassburg, J. Senawirante, N. Dietz, C. J. Summers, and I. T. Ferguson, *Phys. Status Solidi C* **2**, 2441 (2005).
- ⁶Z. S. Popovic, S. Satpathy, and W. C. Mitchel, *Phys. Rev. B* **70**, 161308 (2004).
- ⁷G. Thaler, R. Frazier, B. Gila, J. Stapleton, M. Davidson, C. R. Abernathy, and C. Segre, *Appl. Phys. Lett.* **84**, 1314 (2004).
- ⁸O. Gelhausen, E. Malguth, M. R. Phillips, E. M. Goldys, M. Strassburg, A. Hoffmann, T. Graf, M. Gjukic, and M. Stutzmann, *Appl. Phys. Lett.* **84**, 4514 (2004).
- ⁹B. Han, R. Y. Korotkov, B. W. Wessels, and M. P. Ulmer, *Appl. Phys. Lett.* **84**, 5320 (2004).
- ¹⁰C. Wetzel, E. E. Haller, H. Amano, and I. Akasaki, *Appl. Phys. Lett.* **68**, 2547 (1996).
- ¹¹M. Holtz, T. Prokofyeva, M. Seon, K. Copeland, J. Vanbuskirk, S. Williams, S. A. Nikishin, V. Tretyakov, and H. Temkin, *J. Appl. Phys.* **89**, 7977 (2001).
- ¹²Z. G. Hu, M. B. M. Rinzan, S. G. Matsik, A. G. U. Perera, G. Von Winckel, A. Stintz, and S. Krishna, *J. Appl. Phys.* **97**, 093529 (2005).
- ¹³M. Schubert, T. E. Tiwald, and C. M. Herzinger, *Phys. Rev. B* **61**, 8187 (2000).
- ¹⁴W. Gebicki, J. Strzeszewski, G. Kamler, T. Szyszko, and S. Podsiadlo, *Appl. Phys. Lett.* **76**, 3870 (2000).
- ¹⁵D. Brunner, H. Angerer, E. Bustarret, F. Freudenberg, R. Dimitrov, O. Ambacher, and M. Stutzmann, *J. Appl. Phys.* **82**, 5090 (1997).
- ¹⁶M. B. M. Rinzan, A. G. U. Perera, S. G. Matsik, H. C. Liu, Z. R. Wasilewski, and M. Buchanan, *Appl. Phys. Lett.* **86**, 071112 (2005).